

## Partition of Energy Loss from the Barotropic Tide in Fjords

B. DE YOUNG

*Physical & Chemical Sciences Branch, Scotia-Fundy Region, Department of Fisheries and Oceans,  
Bedford Institute of Oceanography, Dartmouth, Nova Scotia*

S. POND

*Department of Oceanography, University of British Columbia, Vancouver, British Columbia*

4 December 1987 and 1 July 1988

### ABSTRACT

As the barotropic tide propagates into and out of a fjord, it loses energy to friction, internal tides and high-frequency internal waves. Estimates of these losses for three British Columbia fjords, using current meter data, indicate that friction is negligible in two, but important in one inlet. The length and depth of the sill determines the importance of friction. When friction is not important, most of the energy lost goes into the internal tide but less than half of this energy propagates away from the sill. Simple models of the internal tide predict the correct energy transfer to satisfy an energy budget but do not agree with observations of the internal tidal energy flux away from the sill. Energy loss from the internal tide in or near the generation zone would account for the discrepancy. The energy flux of the high-frequency internal wave field is relatively small, about 2% of the energy lost.

### 1. Introduction

As the barotropic tide passes into and out of a fjord, energy is lost. Three potentially important sinks have been identified, the internal tide, bottom friction and high frequency internal waves. There has been some success in estimating one or more of these terms (Stigebrandt 1976; Freeland and Farmer 1980; Webb and Pond 1986; deYoung and Pond 1987), however, no overall energy budget has been developed. Such a budget is important because the energy lost from the barotropic tide can be important within the fjord in driving processes such as vertical mixing and circulation, via nonlinear energy transfer. Following a suggestion of Farmer and Freeland (1983), energy budget analysis also helps in categorizing different fjord processes. On its own, the budget for the energy lost from the barotropic tide may not be sufficient to describe the dynamical nature of a fjord, but it does provide useful information about the dominant energy source. In this paper cyclesonde current meter data are used to provide estimates of energy fluxes in three inlets: Indian Arm, Knight Inlet and Observatory Inlet (see Fig. 1). The focus will be on the first two inlets, for which the most data are available.

In an inlet of arbitrary shape with an identifiable mouth, the Laplace tidal equations are

$$\frac{\partial u}{\partial t} + 2\Omega \times u + g\nabla(\zeta - \zeta_e) - \frac{F}{H} = 0 \quad (1)$$

$$\frac{\partial \zeta}{\partial t} + \nabla \cdot (Hu) = 0 \quad (2)$$

where  $u(x, t)$  and  $\zeta(x, t)$  are velocities and elevations as functions of position,  $H$  is the depth,  $F$  describes the energy losses and  $\zeta_e$  is the equilibrium tide. Following Garrett (1975) and multiplying (1) by  $\rho Hu$  and (2) by  $\rho g \zeta$  one obtains an energy equation which can be averaged over a tidal cycle to obtain

$$\frac{\partial \bar{E}}{\partial t} + \nabla \cdot (\rho g H \bar{u} \zeta) - \rho g H \bar{u} \cdot \nabla \zeta_e = \rho \bar{F} \cdot \bar{u} \quad (3)$$

where  $\rho$  is the density and

$$\bar{E} = \frac{1}{2} \rho H \bar{u}^2 + \frac{1}{2} \rho g \bar{\zeta}^2$$

If  $\partial \bar{E} / \partial t = 0$  and we integrate over the surface area of the fjord, we obtain an equation (Garrett 1975; Farmer and Freeland 1983) representing a balance between the inward flux of tidal energy across the mouth, and outward flux of equilibrium tidal energy, the rate of work by the equilibrium tide on the free surface and the rate of work by frictional forces.

$$-\int_{\text{mouth}} g H \bar{u} \zeta \cdot \bar{n} ds + \int_{\text{mouth}} g H \bar{u} \zeta_e \cdot \bar{n} ds + \int_{\text{mouth}} g \zeta_e \frac{\partial \zeta}{\partial t} dA = \int_{\text{area}} \bar{F} \cdot \bar{u} dA. \quad (4)$$

Corresponding author address: Dr. Brad deYoung, Dept. of Physics, Memorial University, St. John's, Newfoundland A1B 3X7.

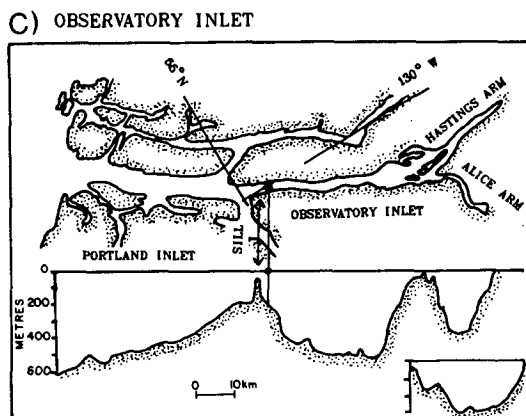
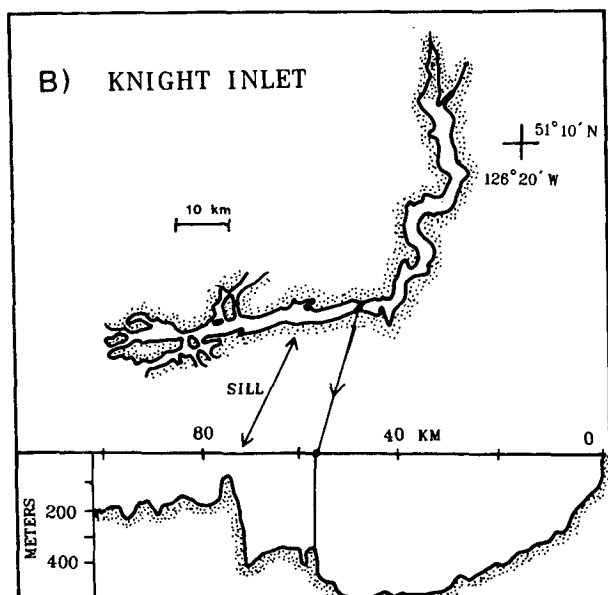
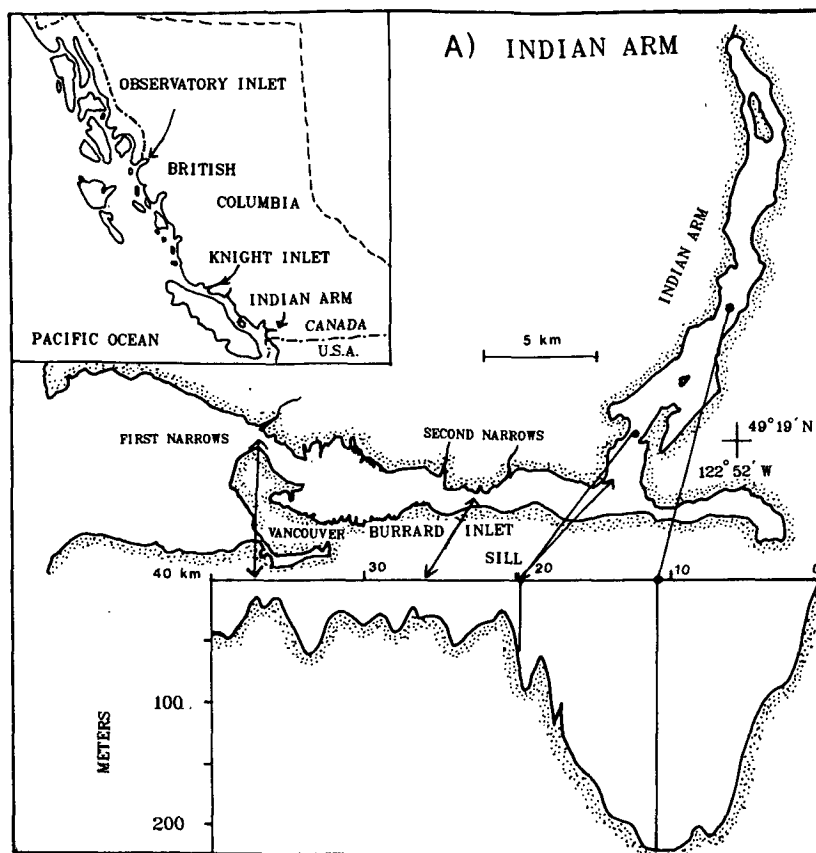


FIG. 1. Area maps for the three inlets discussed. Positions of the cyclesonde current meter moorings are indicated with a dot on the plan view map and a vertical line on the side view of the bottom topography. (a) Indian Arm, showing the basin and Burrard Inlet, which acts as an extended sill for the fjord. The two sills in Burrard Inlet are at First and Second Narrows. (b) Knight Inlet showing the cyclesonde mooring position and along-channel topography. (c) Observatory Inlet and the cyclesonde mooring position just inside the sill.

In (4)  $\mathbf{n}$  is the normal perpendicular to an element  $ds$  at the mouth. The middle terms can be consolidated to yield a single term which is small in fjords (Farmer and Freeland 1983) yielding

$$-\int_{\text{mouth}} gHu\zeta \cdot \mathbf{n} ds = \int_{\text{area}} \overline{F \cdot u} dA. \quad (5)$$

The balance is between work done by the tide and energy loss processes, which are not defined in (5). We consider energy transfer to the internal tide, bottom friction and high frequency internal waves. Velocity and elevation are approximately in quadrature, however, two factors make it difficult to use the left side of (5) directly to compute the total energy transfer from the tide. In the absence of dissipation, velocity and elevation are in quadrature. Because current meters are noisy instruments and internal tides are present which contaminate the current signal, it is difficult to use elevation and current data directly to compute energy loss. Freeland and Farmer (1980) show that the dissipation in an arbitrary section can be determined from

$$P = \frac{1}{2} \rho g \zeta_0^2 \omega B l \sin \epsilon \quad (6)$$

where  $\zeta_0$  is the amplitude of a harmonic of the elevation of frequency  $\omega$ ,  $B$  the channel width,  $l$  the length of the inlet and  $\epsilon$  the phase difference between the surface elevation and the velocity. It is not possible in general to measure  $\epsilon$  which can, however, be determined from phase changes in the surface elevation along the inlet (Freeland and Farmer 1980; deYoung and Pond 1987). To get  $\epsilon$  from along-inlet phase changes, the inlet is assumed to be of uniform shape. In this paper we are interested in the loss terms from the barotropic tide.

Some of the energy loss is influenced by stratification (internal tides, internal waves) while other energy loss from the barotropic tide is comparatively independent of the density regime (friction). Internal tides are generated on both sides of the sill in a fjord (Rattray 1960; Webb and Pond 1986; deYoung and Pond 1987) and over the sloping shore near the head of the fjord (Farmer and Osborn 1976). Nonlinear tidal effects are indicated by the presence of tidal harmonics (Blackford 1978; Stigebrandt 1980) and shallow water tidal constituents. Such nonlinear effects are important in Observatory and Knight inlets (Freeland and Farmer 1983) but not in Indian Arm where tidal harmonics are not found. Seasonal variations in the energy loss from the barotropic tide in Knight Inlet (Freeland and Farmer 1980) and Observatory Inlet (Stacey 1984) indicate the influence of stratification on the energy transfer to internal processes.

Freeland and Farmer (1980) have also made estimates of the bottom friction term in Knight Inlet concluding that it could only account for about 3% of the energy lost from the barotropic tide. All of these inlets are relatively narrow (1–5 km) so side friction may be

important, particularly in the deep basins, but over the sill where frictional loss will be greatest, the depth over the width is small, of order 100/1000  $\sim$  0.1. In Observatory Inlet, Stacey (1984) estimates the frictional loss to be 1–2% of the energy lost by the barotropic tide. Estimates of the energy flux in the high-frequency internal waves have not been made before although there have been numerous studies of their dynamics and structure (Farmer and Smith 1980a,b; Farmer and Freeland 1983). Stacey and Zedel (1986), using the nonlinear shallow water equations applied to three-layer flow over the sill of Observatory Inlet, suggest that only 5% of all of the energy removed from the barotropic tide goes into hydraulic flow phenomena (i.e. hydraulic jumps, high-frequency internal waves). They suggest that most of the energy withdrawn from the barotropic tide goes into the internal tide. One goal of this paper is to use observations in different fjords to test their suggestion.

## 2. Data description

The cyclesonde current meter data were collected with the purpose of obtaining good information on the vertical structure of the observed currents (Webb and Pond 1986; deYoung and Pond 1987). The cyclesonde is a profiling current meter CTD system (Van Leer et al. 1974), which profiles up and down a taut wire subsurface mooring, sitting at a bumper at the top or bottom of the mooring between profiles. The sampling rate is 1 minute when profiling. The sampling rate remains at 1 minute after the profile, while at the top or bottom bumper, for up to one-half hour and then changes to 5-minute sampling. Observations of high-frequency internal waves at the two bumpers will therefore be aliased to some extent; however, it is still expected that a reasonable estimate of the variance in this frequency band (2–30 cph) can be obtained.

## 3. Energy flux estimates

### a. Indian Arm

Indian Arm is a narrow (1.3 km) and relatively short (22 km) inlet (deYoung and Pond 1988). It has an average depth of 200 m in the basin, with a sill at 26 m. It is connected to the Strait of Georgia by a narrow (0.5–2 km) and shallow (15–60 m) channel, Burrard Inlet, which acts as an extended (20 km) sill for Indian Arm. Indian Arm is a low runoff inlet with weak winds in summer and in winter, thus making it a good location to study energy processes associated with the barotropic tide because of the weakness of other forcing. It is unusual, compared to the two other inlets under discussion, in that there is both a strong  $M_2$  and  $K_1$  internal response depending upon the stratification (deYoung and Pond 1987). The energy loss from the barotropic tide was determined from the phase change of the surface elevation along the inlet using the method

of Freeland and Farmer (1980). Pressure data from tide gauges and cyclesondes were used to determine the phase change of the surface elevation along the inlet (deYoung and Pond 1987) for the winters of 1983/84 and 1984/85.

The energy flux of the internal tide was found by using two techniques. Normal modes, determined from the density structure, were fitted to the cyclesonde density and current data. The results presented here are an average of the 1983/84 and 1984/85 winters. Both current and density data were used to allow determination of the up- and down-inlet fluxes (deYoung and Pond 1987). The net energy flux was also found by direct calculation, for 1985 when observations over the whole water column were available, by integrating the time average product of the perturbation pressure and the velocity associated with the internal motion,  $\langle p'u \rangle$  (Gill 1982), over the width and the depth. The modal technique yields the flux in each direction while the perturbation technique gives the net flux at a point.

The top line in Table 1 gives the tidal energy flux at the sill of Indian Arm, about 0.5 km away from the cyclesonde mooring position shown in Fig. 1a. About 3% (0.7 MW) of the total incoming energy, of both the  $M_2$  and  $K_1$  tidal constituents, is lost in Indian Arm. A much larger amount of energy is lost upstream through Burrard Inlet. At each of the two sills in Burrard Inlet about 4.5 MW is lost, corresponding in total to about 18% of the barotropic tidal flux entering Burrard Inlet at First Narrows (deYoung and Pond 1987). Note that for both areas about the same percentage of energy is lost from each of the two dominant tidal constituents. The internal tide generated at the sill is strongly dissipated as it moves up-inlet. At the basin station (about 8 km from the sill station, see Fig. 1a), the internal tide is reduced by a factor of 2–5. The two different flux calculation methods show approximate agreement at the sill, good for  $K_1$ , not so good for  $M_2$ . The difference between the two techniques may be partially ascribed to the fact that the perturbation calculation gives a net energy flux. Also the perturbation calculation is done for just two months from the winter of 1984/85. The modal flux calculation is an average of seven months of data from the 1983/84 and 1984/85 winters.

The kinetic energy spectrum is continuous with distinct tidal peaks present. By high frequency energy, we

TABLE 1. Energy fluxes (in MW) in Indian Arm.

	$M_2$	$K_1$
Energy entering Indian Arm	16	7
Energy lost in Indian Arm	0.5	0.2
Upchannel flux from modal fitting		
Sill	0.15	0.05
Basin	0.03	0.02
Net flux from $\langle p'u \rangle$ at the sill in 1985	~0.05	~0.05
HF internal wave flux		~0.02
Energy lost to friction		~0.4
Energy lost to mixing		~0.05

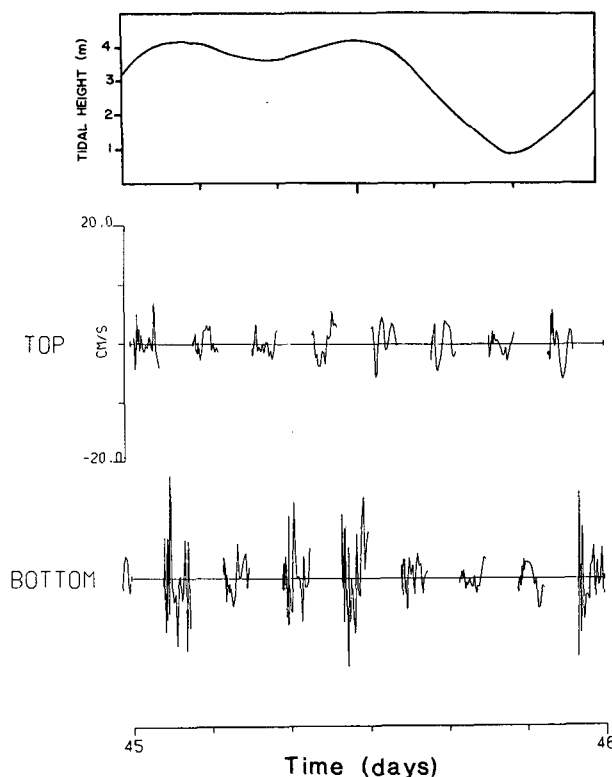


FIG. 2. Along-channel current velocities inside the Indian Arm sill in 1985. Time is in Julian days. The nominal depths are Top (14–20 m) and Bottom (60–66 m). The tide has been removed from the entire record. The mean and trend have been removed from each individual block of data. The gaps occur when the instrument was profiling or sitting at the other bumper. The tidal height plot is of observed data from a station in Burrard Inlet, about 18 km from the current meter mooring.

refer to periods below one hour. This term will be estimated from the variance about one hour means in the along-channel velocity, using the current data from the cyclesonde when sitting at the top and bottom bumper. The resulting time series has gaps, when the instrument was profiling or at the other bumper, and a changing sampling rate (1 or 5 minutes). Using harmonic analysis, the tidal signal is removed. The mean and trend are removed from the short blocks of data, each of which is about one hour in length. A sample of the resulting along-channel velocity signal (Fig. 2) shows that waves of 5–20 minute period are present. From the tidal height curve in Fig. 2 it can be seen that increased high-frequency wave energy is associated with the flood tide, while reduced high-frequency activity is associated with ebb tides. The variance of each block of data is computed and an average variance calculated for the top and bottom. The energy flux is computed from the averaged variance using

$$\text{Flux} = \rho_0 Cg [A_{\text{TOP}} \text{var}_{\text{TOP}} + A_{\text{BOT}} \text{var}_{\text{BOT}}] \quad (7)$$

where  $\rho_0$  is the average density,  $Cg$  is the group velocity  $[(g(\rho_2 - \rho_1)/\rho_2)(h_1 h_2 / (h_1 + h_2))]^{1/2}$ ,  $A$  the cross-sectional

area at the current meter station and *Var* the average energy density. TOP indicates data from the top bumper (14–20 m subsurface), BOT data from the bottom bumper (~10 m above bottom). The depths  $h_1$  and  $h_2$  represent upper and lower layer depths and were determined from the density profiles (deYoung and Pond 1988). Three months of current meter data (February 1984, January 1985 and February 1985) were analyzed, from a point less than one km inside the Indian Arm sill. The group velocity, estimated from the density structure, is  $\sim 0.5 \text{ m s}^{-1}$ . The high-frequency flux (0.02 MW) is comparable to the internal tidal flux in the basin, though not at the sill. It represents about 3% of the energy lost from the barotropic tide.

If these flux estimates are correct then there is some missing energy. The remaining term to estimate is the frictional loss which can be estimated using a formula derived by Freeland and Farmer (1980)

$$\rho_0 K \int U^3 ds \quad (8)$$

where  $K$  is a dimensionless drag coefficient set at  $3 \times 10^{-3}$ ,  $U$  is the mean velocity and the integration is over the area of the sill. The frictional loss is assumed to take place at the bottom. Taking the area of the sill ( $ds$ ) as  $1 \text{ km}^2$  and a depth-averaged flow speed of  $0.5 \text{ m s}^{-1}$  gives a frictional loss of 0.4 MW. Including friction, the total flux at the sill is 0.62 MW, agreeing very well with the observed loss of 0.7 MW and approximately closing the energy budget. Most of the energy lost over the Indian Arm sill appears to go into friction, almost 60%, with the remainder going into the internal tide.

The final line in Table 1 gives the estimated energy loss to mixing. The flux is the integral of  $K_v N^2$  over the volume of the fjord (Stigebrandt 1980). The coefficient of vertical diffusivity is determined from a salinity budget study (deYoung and Pond 1988). Only a small percentage (~7%) of the energy lost from the barotropic tide does work against buoyancy.

### b. Knight Inlet

Knight Inlet is roughly 100 km long with an average width of 2.5 km. The mean annual freshwater discharge is  $400 \text{ m}^3 \text{ s}^{-1}$ . The  $M_2$  tide dominates in Knight Inlet with nonlinear interactions generating higher order harmonics (Farmer and Freeland 1983). Knight Inlet is a much more tidally energetic inlet than Indian Arm. In addition, both the wind driven and freshwater circulation are much more prominent (see Farmer and Freeland 1983). It thus provides an interesting contrast to Indian Arm. The techniques used to determine the fluxes in Indian Arm in the previous section are used once again.

The energy withdrawal from the barotropic tide in Knight Inlet is seasonal, from 4–9 MW depending on

the stratification. The greatest loss occurs during the period of maximum stratification. The total energy lost from the barotropic tide during late summer is about 7 MW, roughly 2% of the incoming energy (Table 2). For the high-frequency wave analysis, three records, each one month long from 18 km inside the sill are used [July 1983 (two records) and September 1983]. The bumper depths are 15–20 m and 175–180 m with a total water depth of 340 m.

The station position in Knight Inlet corresponds to the basin station of Indian Arm in that it is away from the sill (Fig. 1b). The high-frequency flux at this station within the basin is probably less than would be observed closer to the sill. The group velocity, determined from the density conditions, is  $0.5 \text{ m s}^{-1}$ . Very little energy is transferred to high-frequency internal waves (~0.1 MW). Freeland and Farmer (1980) argue that only about 3% (~0.2 MW) of the energy lost goes into friction. The majority of the energy loss appears in the internal tide, ~2.8 MW (Webb and Pond 1986), about 40% of the total lost. The estimated internal tidal flux of Webb and Pond (1986) is about half that predicted by Stacey's (1984) linear model. One explanation for the discrepancy is that a lot of the internal tidal flux does not make it away from the generation zone in the neighbourhood of the sill. This is precisely what is observed in Indian Arm where one of the cyclesondes is in the middle of the generating region. In the sill region a great deal of energy may be transferred from the barotropic tide to the internal tide and then to other nonlinear motions, at higher frequencies perhaps, which do not propagate far from the sill region.

### c. Observatory Inlet

Although roughly equal in surface area, the  $M_2$  tidal amplitude range in Observatory Inlet (2 m) is greater than that in Knight Inlet (1.5 m). The barotropic energy flux in Observatory Inlet is therefore almost twice that in Knight Inlet (Table 3). As in Knight Inlet the barotropic tidal loss in Observatory Inlet shows seasonal variability (Stacey 1984). The energy loss varies from 9 to 25 MW, the maximum occurring during the period of greatest stratification. Stacey shows that most of the energy loss can be explained using a simple linear model, which is an extension of a model of Stigebrandt (1976, 1980). The energy withdrawn from the tide in late summer (25 MW) is a much larger percentage (~4%) of the total than determined in Knight Inlet (2%). This difference may be caused by the local con-

TABLE 2. Energy fluxes (in MW) in Knight Inlet.

$M_2$ energy entering at the sill	370
Energy lost from the $M_2$ tide	4–9
Flux from modal fitting	2.8
HF internal wave flux	0.1
Frictional loss	0.2

TABLE 3. Energy fluxes (in MW) in Observatory Inlet.

$M_2$ energy entering at the sill	612
Energy lost from the $M_2$ tide	9–25
Calculated internal tidal flux	8–24
HF internal wave flux	0.4
Friction over the sill	0.2

ditions, that is, the stratification and bottom topography promote a more efficient transfer of energy to the internal tide, or it may be related to stronger nonlinear effects over the Observatory Inlet sill. Stacey (1984) estimated the frictional loss at 0.2 MW, a small number, so it does not appear that the extra energy lost is going into friction. Stacey (1984) and Stacey and Zedel (1986) found that most of the energy loss could be accounted for by both linear and nonlinear models. The high-frequency energy flux (0.4 MW), using a group velocity of  $1.0 \text{ m s}^{-1}$ , is greater than the frictional loss but still much smaller than the total flux withdrawn from the barotropic tide. For the high-frequency flux in Observatory Inlet only top bumper data (15–20 m depth) for a single month, August 1982, were available. The station used for the high-frequency flux analysis is about 2 km inside the Observatory Inlet sill (Fig. 1c). It should be noted here that the internal tidal fluxes discussed here are theoretically determined (Stacey 1984) and not measured directly although there are some measurements confirming the theoretical estimates. Thus the energy flux which actually makes it a significant distance away from the sill, say a half-wavelength ( $\sim 10 \text{ km}$ ) or more, may indeed be much smaller than that predicted by the present models, as is the case in Knight Inlet.

#### 4. Discussion and conclusions

In all three inlets, the energy lost from the barotropic tide is small, ranging from 2% in Knight Inlet to 4% in Observatory Inlet. Most of the barotropic energy is reflected out of the inlet. Burrard Inlet differs in that about 18% of the barotropic energy entering at First Narrows is lost, with about the same amount (9%) being lost at each sill (First and Second Narrows) in Burrard Inlet (deYoung and Pond 1987). Friction appears to dominate in Burrard Inlet because of the extent of the shallow (15–20 m) sills. In Knight and Observatory inlets, direct loss of barotropic tidal energy to friction is small and this result is probably generally true for all fjords with short sills. Indian Arm has an extensive rather shallow sill and the frictional loss is significant, about one half of the total loss. Except for unusual cases like Burrard Inlet, one may expect that the loss of barotropic tidal energy in fjords will be only a few percent as in Indian Arm, Knight and Observatory Inlets. While the percentage loss from the barotropic tide is small, the amount of energy is large in relation to the overall fjord energy budget. Indeed, it is usually

the dominant energy source (Farmer and Freeland 1983).

In all three cases energy transfer to internal tides is an important sink for barotropic tidal energy. In fact, in Knight and Observatory inlets the model of Stacey (1984) predicts that virtually all of the transfer is to internal tides and the predicted loss follows the seasonal cycle of the observed loss rather well. Some distance away from the sill, however, the energy flux in the internal tides is considerably smaller than the energy extracted from the barotropic tide. Either the generation mechanism is more complicated or dissipation of the internal tide near the sill is rapid and further investigation is warranted. In either case any inward propagating internal tidal energy is likely to remain within the inlet, particularly if the sill is shallow (Robinson 1969).

The direct estimates of the high-frequency internal wave energy flux reported here show that it is small compared to the energy flux out of the barotropic tide. Our estimates could be somewhat low if the energy flux is larger in the near-surface layer which we have not sampled. Even if the flux is larger there, it is not likely to significantly change these results since the high-frequency flux would still be a small term even if it were doubled. Measurements in the near-surface layer are needed, however, to check the importance of this region.

One check of the robustness of our energy flux estimates is to attempt a closure of the energy budget. Only for Indian Arm, where there are internal tidal flux estimates near the sill, are there enough data to test the energy budget. The sum of the internal tidal flux near the sill (0.2 MW), friction over the sill (0.4 MW) and high-frequency internal waves near the sill (0.02 MW) is 0.62 MW. This energy flux total compares well with the observed energy loss from the barotropic tide (0.7 MW).

Except for internal waves of tidal and shorter period generated on the seaward face of the sill, which may radiate energy away, most of the energy lost from the barotropic tide remains in the inlet eventually to be dissipated or to contribute to mixing, whatever the pathway of the loss. The energy going into mixing will be small as turbulent mixing is inefficient, perhaps even more so in fjords because there are intermediate (internal) motions generated during the transfer from the barotropic tide. We calculated a 7% transfer to mixing in Indian Arm, Stigebrandt (1980) estimates 5% for Oslofjord.

*Acknowledgments.* We thank M. Stacey for discussion of internal tidal models, and the many people at UBC who provided technical assistance, in particular V. Lee who helped with much of the computer analysis of the cyclesonde data. J. Loder and S. Prinsenberg provided internal reviews of the manuscript which M. Burhoe and P. Roy typed.

## REFERENCES

- Blackford, B. L., 1978: On the generation of internal waves by tidal flow over a sill—a possible nonlinear mechanism. *J. Mar. Res.*, **36**, 529–549.
- deYoung, B., and S. Pond, 1987: The internal tide and resonance in Indian Arm, British Columbia. *J. Geophys. Res.*, **92**, 5191–5207.
- , 1988: The deepwater exchange cycle in Indian Arm, British Columbia. *Estuarine Coastal Shelf. Sci.*, **26**, 285–308.
- Farmer, D. M., and H. J. Freeland, 1983: The physical oceanography of fjords. *Progress in Oceanography* Vol. 12, Pergamon, 147–220.
- , and T. R. Osborn, 1976: The influence of wind on the surface layer of a stratified inlet. Part I. Observations. *J. Phys. Oceanogr.*, **6**, 931–940.
- , and J. D. Smith, 1980a: Tidal interaction of stratified flow with a sill in Knight Inlet. *Deep-Sea Res.*, **27A**, 239–254.
- , 1980b: Generation of the waves over the sill in Knight Inlet. *Fjord Oceanography*. H. J. Freeland, D. M. Farmer and C. D. Levings, Eds., Plenum Press, 259–269.
- Freeland, H. J., and D. M. Farmer, 1980: Circulation and energetics of a deep, strongly stratified inlet. *Can. J. Fish. Aquatic Sci.*, **37**, 1398–1410.
- Garrett, C. J. R., 1975: Tides in gulfs. *Deep-Sea Res.*, **22**, 23–36.
- Gill, A. E., 1982: *Atmosphere-Ocean Dynamics*. Academic Press, 662 pp.
- Ratray, M., Jr., 1960: On the coastal generation of internal tides. *Tellus*, **12**, 54–62.
- Robinson, R. M., 1969: The effects of a vertical barrier on internal waves. *Deep-Sea Res.*, **16**, 421–429.
- Stacey, M. W., 1984: The interaction of tides with the sill of a tidally energetic inlet. *J. Phys. Oceanogr.*, **14**, 1105–1117.
- , and L. J. Zedel, 1986: The time dependent, hydraulic flow over the sill of Observatory Inlet. *J. Phys. Oceanogr.*, **16**, 1062–1076.
- Stigebrandt, A., 1976: Vertical diffusion driven by internal waves in a sill fjord. *J. Phys. Oceanogr.*, **6**, 486–495.
- , 1980: Some aspects of tidal interaction with fjord constrictions. *Estuarine Coastal Mar. Sci.*, **11**, 151–166.
- Van Leer, J. C., W. Duing, R. Enath, E. Kennelly and A. Speidel, 1974: The Cyclesonde: An unattended vertical profiler for scalar and vector quantities in the upper ocean. *Deep-Sea Res.*, **21**, 385–400.
- Webb, A. J., and S. Pond, 1986: A modal decomposition of the internal tide in a deep, strongly stratified inlet: Knight Inlet, British Columbia. *J. Geophys. Res.*, **91**, 9721–9738.